Volume 308, number 2, 190–196 FEBS 11425 August 1992

Three-dimensional structure of (1–36)bacterioopsin in methanol–chloroform mixture and SDS micelles determined by 2D ^{1}H-NMR spectroscopy

Konstantine V. Pervushin and Alexander S. Arseniev

Shemyakin Institute of Bioorganic Chemistry, Russian Academy of Sciences, Moscow, Russia

Received 18 June 1992

Spatial structures of proteolytic segment A (sA) of bacterioopsin of *H. halobium* (residues 1–36) solubilized in a mixture of methanol–chloroform (1:1), 0.1 M $LiClO_4$ organic mixture, or in perdeuterated sodium dodecyl sulfate (SDS) micelles, were determined by 2D ^{1}H-NMR techniques. 324 and 400 NOESY cross-peak volumes were measured in NOESY spectra of sA in organic mixture and SDS micelles, respectively. The sA spatial structures were determined by local structure analysis, distance geometry calculation with program DIANA and systematic search for energetically allowed side chain rotamers consistent with NOESY cross-peak volumes. The structures of sA are similar in both milieus and have the right-handed α-helical region from Pro^8 to Met^{32} with root mean square deviation (RMSD) of 0.25 Å between backbone heavy atoms and fit well with Pro^8 to Met^{32} α-helical region in electron cryo-microscopy model of bacteriorhodopsin. The N-terminal region Ala^2–Gly^6 of sA in organic mixture has a fixed structure of two consecutive γ-turns as 2_1-helix (RMSD of 0.25 Å) stabilized by the Thr^3 NH···O=C Gln^5 and Ile^4 NH···O=C Ala^2 hydrogen bonds while this region in SDS micelles has disordered structure with RMSD of 1.44 Å for backbone heavy atoms. The C-terminal region Gly^{33}–Asp^{36} of sA is disordered in both milieus. Torsion angles χ^1 of sA were unequivocally determined for 13 (SDS) and 11 (organic mixture) of α-helical residues and are identical in both milieus.

NMR; Distance geometry; Micelle; Bacterioopsin; Spatial structure

1. INTRODUCTION

Bacteriorhodopsin (BR) is a transmembrane protein of 248 amino-acid residues, which acts as a light-driven proton pump in the purple membrane of *Halobacterium halobium* (for review see [1]). According to the latest model of BR from electron cryo microscopy (ECM) data, the spatial structure of the molecule consists of seven transmembrane α-helices A–G packed together [2]. This model providing description of general fold of BR is not reliable on the atomic level because of low resolution of ECM.

NMR spectroscopy is a powerful technique for the elucidation of the spatial structure of water-soluble proteins with a molecular mass of up to 30 kDa [3]. Unfortunately, the resonances in NMR spectra of a membrane protein incorporated in the bilayer membrane or small liposomes are too broad to be resolved individually. Therefore the choice of an artificial medium conserving the protein structure and providing high-resolution NMR spectra is crucial for such studies. Due to the limits of two dimensional (2D) ^{1}H-NMR methods organic solvents or detergent micelles are used as membrane mimicking milieus. The detailed conformation of BR fragments in membrane mimicking milieus can be obtained by 2D ^{1}H-NMR spectroscopy, and these fragments might be regarded as natural blocks as a basis of BR spatial structure reconstruction. Previously, the secondary structure was determined for bacterioopsin synthetic transmembrane segments B (residues 34–65) [4,5], D (residues 102–136) [6], G (residues 205–231) [7] and proteolytic fragments BP2 (residues 163–231) [8] and C2 (residues 1–71) [9] solubilized in methanol–chloroform (1:1), 0.1 M $LiClO_4$. Segment B was also studied in sodium dodecyl-d_{25} sulfate (SDS) micelles [10,11]. Here we present the comparison of segment A (residues 1–36) spatial structures in methanol–chloroform (1:1), 0.1 M $LiClO_4$ and SDS-d_{25} micelles determined from NMR data, while the proton resonance assignments and analysis of secondary structures will be published in [12]. The strategy for sA spatial structure calculation is similar to that used for segment B in detergent micelles [11].

Abbreviations: BR, bacteriorhodopsin; sA, (1–36)bacterioopsin; ECM, electron cryo microscopy; 2D, two-dimensional; NOESY, 2D homonuclear NOE spectroscopy; RMSD, root mean square deviation.

Correspondence address: A.S. Arseniev, Shemyakin Institute of Bioorganic Chemistry, Russian Academy of Sciences, Ul. Miklukho-Maklaya 16/10, Moscow, 117971, Russia. Fax: (7) (095) 310-7007.

2. MATERIALS AND METHODS

2.1. *NMR measurements and input data for spatial structure computation*

The proteolytic fragment (1–36) bacterioopsin (sA) was isolated as described in [13]. Two-dimensional ^{1}H-NMR NOESY (relaxation

Published by Elsevier Science Publishers B.V.

delay of 1.2 s and mixing time of 150 ms) and TOCSY (mixing time of 45 ms) spectra of 3 mM solution of sA in C^2H_3OH/C^2HCl_3 (1:1), 0.1 M $LiClO_4$ or in 0.24 M SDS-d_{25} in H_2O in the presence of trifluoroethanol-d_3 (TFE-d_3) (20% by volume) were recorded at 600 MHz (Varian Unity 600 spectrometer) at 35°C. NOESY cross-peak volumes were measured by a curve fitting procedure [14]. Nonselective spin lattice relaxation times (T_1) of individual protons were measured by the inversion-recovery method.

Theoretical NOESY cross-peak volumes expected for a conformation of sA were calculated by diagonalization of the complete relaxation matrix and corrected in accordance with proton relaxation times T_1 as described in [15]. For correction we used mean T_1's for each group of protons: 1.0 s, indole NIH protons; 0.75 s, backbone NH protons; 1.3 s, aromatic protons and 0.6 s, other side chain protons.

The integration of the NOESY spectrum of sA in SDS micelles or organic mixture gave volumes for 400 and 324 cross-peaks, respectively. 282 and 258 cross-peaks were unambiguously assigned and used to derive a set of constraints for distance geometry calculations with the program MARDIGRAS [16]. Among them there are 88 (SDS) and 57 (organic mixture) sequential and 83 (SDS) and 74 (organic mixture) medium-range ($1 < |i-j| \leq 4$, where i,j are residue numbers) cross-peaks. The long-range ($|i-j| > 4$) were not presented in NOESY spectra. Obtained patterns of NOE connectivities are shown in Fig. 1. Also 42 (SDS) and 36 (organic mixture) distance restraints were used to define 21 and 18 hydrogen bonds within the α-helical region (residues 8–32) that were identified based on both NOE's and amide protons deuterium exchange data (Fig. 1) [12]. Preliminary structure calculations without inclusion of the hydrogen-bond restraints have shown the predicted hydrogen bonds to be quite compatible with the experimentally derived distance constraints.

2.2. *Computation of sA spatial structure*

The reconstruction of sA spatial structure includes the following steps: (1) analysis of the local structure and evaluation of the effective rotational correlation time with the program CONFORNMR [11,17], (2) structure calculation with the distance geometry program DIANA [18], (3) the systematic search for allowed side chain rotamers consistent with NOESY cross-peak volumes using program CONFORNMR, (4) DIANA calculations with additional constraints on the torsion angles of side chains obtained at stage 3, and (5) unrestrained energy minimization with the program CONFORNMR using the ECEPP/2 force field [19].

The local structure of sB was analyzed using the $F_i(\varphi,\psi,\chi,\tau_c)$ dependencies [17] for each dipeptide unit i of the polypeptide included all protons of residue i and amide proton of residue $i+1$. The correlation time τ_c was determined as a minimum of $F_i(\tau_c)$ dependence for each dipeptide unit, where $F_i(\tau_c)$ is a global minimum value of $F_i(\varphi,\psi,\chi)$ at a given τ_c. For sA in SDS micelles the optimum value of τ_c was within the range of 5–7 ns for most dipeptide units, while this time for sA in organic mixture was within 4–6 ns, so in further computations we used the mean values of correlation times τ_c of 6 and 5 ns, respectively. As results we obtained 28 (SDS) and 31 (organic mixture) restraints on φ and ψ angles and also 32 (SDS) and 31 (organic mixture) restraints on χ^1 and χ^2 angles.

Structures were calculated using the program DIANA [18] by optimizing randomly generated starting conformations according to standard protocol. Special attention was paid to the Ala^3-Gly^6 region of sA in the organic mixture, where slow deuterium exchange of amide protons was detected and NOE pattern does not correlate with regular α-helix (Fig. 1).

The allowed side chain conformations in the region 8–32 with the defined α-helical backbone structure can be found when comparing the penalty functions F_i and relative conformational energy ΔE for all possible side chain rotamers of the given residues [11,17]. We chose DIANA conformation with the lowest value of the penalty function as a starting one, but the results were not dependent on the start. The starting sA conformation was refined using energy minimization by CONFORNMR [17] with ECEPP/2 parameters [19]. Then for each residue i all side chain rotamers were considered with the energy

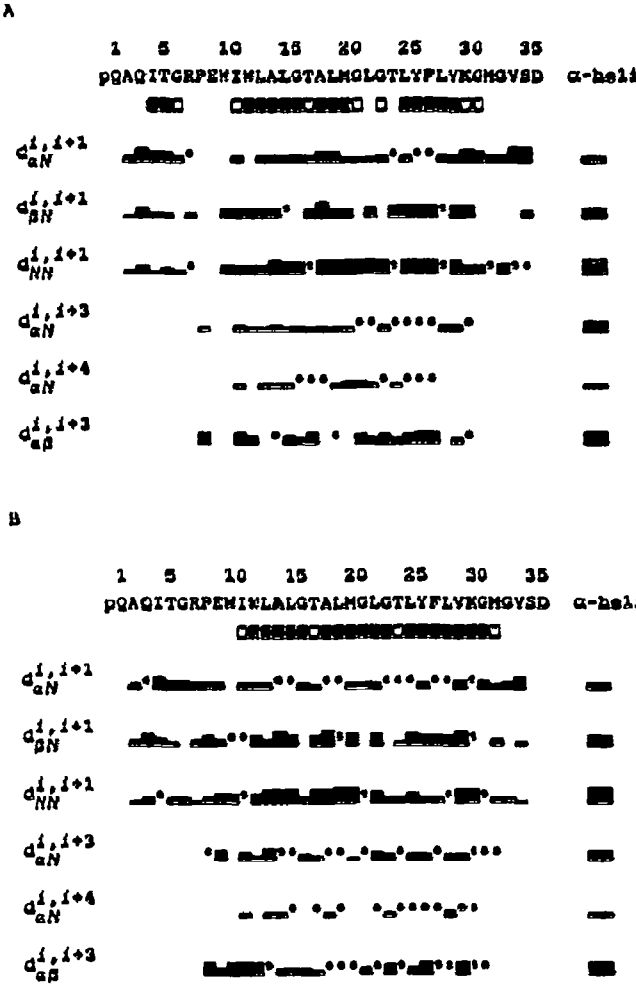

Fig. 1. Amino-acid sequence of (1–36)bacterioopsin and survey of the NOE connectivities in (a) methanol-chloroform, 0.1 M $LiClO_4$ solution and (b) SDS-d_{25} micelles; pQ denotes pyroglutamic acid residue. The thickness of lines corresponds to cross-peak volumes and rightmost column shows the NOE pattern expected for a residue in the canonical right-handed α-helix. Overlapping cross-peaks are denoted by filled circles. Residues with slowly exchanging amide protons are indicated by filled squares and those presented only in the first of sets of 2D NOESY spectra used to determine deuterium exchange rates of amide protons indicated by open squares.

minimization and penalty function evaluation for the region $i \pm 5$ of the α-helix. All rotamers with $F_i < F_i^{min} + 0.1$ Å (where F_i^{min} is minimum value F_i for side chain rotamers of the given residue i) were considered in agreement with NOESY cross-peaks volumes. If several rotamers met the above conditions we used conformational energy as an additional criterion and selected only rotamers with the energy less than 5 kcal/mol relative to the lowest energy for the $i \pm 5$ region. All allowed side chain rotamers determined at this stage are listed in Table I.

The final sets of sA conformations were generated using DIANA with additional constraints on χ^1 and χ^2 torsion angles coming from the previous stage. The variation of φ and ψ angles, which characterize the quality of the obtained backbone structure is presented in Fig. 2.

3. RESULTS AND DISCUSSION

The sets of the 16 best DIANA conformations of sA in organic mixture or SDS micelles with final target

Table I

Penalty functions F_r (Å) and relative energies ΔE (kcal/mol) calculated for the $i \pm 5$ region with g⁺, g⁻ and t rotamers of C^{α}–C^{β} bond of residue i, amounts of NOESY cross-peaks (N) used for calculation of F_r and allowed side chain rotamers of C^{α}–C^{β} bond found for the 9–32 region of sA in methanol–chloroform (1:1), 0.1 M $LiClO_4$ (upper line) and SDS-d_{25} micelles (lower line)

Residue	F_r (Å)			ΔE (kcal/mol)			N	Allowed rotamer
	g⁺	g⁻	t	g⁺	g⁻	t		
Glu⁹	–	–	–	–	–	–	–	
	0.08	0.23	0.10	1.2	5.6	0.0	5	g⁺,t
Trp¹⁰	0.32	0.47	0.29	7.4	18.9	0.0	7	t
	0.65	0.93	0.17	2.6	26.1	0.0	9	t
Ile¹¹	0.15	0.61	0.46	0.0	10.4	0.9	13	g⁻
	0.09	0.52	0.42	0.0	7.0	5.0	17	g⁻
Trp¹²	0.09	0.24	0.10	8.3	17.4	0.0	8	t
	0.14	0.65	0.06	5.4	18.4	1.8	10	t
Leu¹³	0.34	0.23	0.19	1.9	13.9	0.0	5	t
	0.14	0.41	0.06	1.7	14.3	0.0	12	t
Leu¹⁵	0.12	0.32	0.24	1.5	6.4	0.0	5	g⁻
	0.15	0.57	0.09	1.5	7.2	0.0	6	g⁻,t
Thr¹⁷	0.08	0.34	0.36	0.0	6.5	10.0	10	g⁻
	0.10	0.37	0.40	0.0	3.8	7.1	7	g⁻
Leu¹⁹	0.03	0.37	0.04	1.1	11.0	0.0	2	g⁻,t
	0.53	0.58	0.10	0.0	12.0	0.6	5	t
Met²⁰	0.20	0.36	0.17	1.2	5.2	0.0	7	g⁻,t
	0.09	0.33	0.57	1.4	5.4	0.0	16	g⁻
Leu²²	0.16	0.28	0.35	0.6	4.9	0.0	7	g⁻
	0.11	0.31	0.02	2.1	5.1	0.0	6	t
Thr²⁴	0.20	0.45	0.69	0.0	6.8	11.1	12	g⁻
	0.14	0.30	0.42	0.0	4.1	10.2	4	g⁻
Leu²⁵	0.14	0.30	0.18	0.0	14.1	0.6	11	g⁻,t
	0.15	0.32	0.06	1.7	7.0	0.0	6	t
Tyr²⁶	0.82	0.37	0.21	0.0	10.0	2.4	19	t
	0.86	0.79	0.06	2.7	11.0	0.0	9	t
Phe²⁷	0.48	0.50	0.21	1.6	8.3	0.0	6	t
	0.50	0.40	0.02	1.9	10.0	0.0	3	t
Leu²⁸	0.11	0.89	0.11	0.8	14.8	0.0	2	g⁻,t
	0.28	0.50	0.29	0.7	8.3	0.0	10	g⁻,t
Val²⁹	0.33	0.38	0.29	10.2	6.8	0.0	12	t
	0.20	0.24	0.23	9.9	7.5	0.0	14	t
Lys³⁰	0.33	0.69	0.29	2.2	5.7	0.0	13	g⁻,t
	0.20	0.26	0.36	0.8	3.5	0.0	9	g⁻,g⁻,t
Met³²	0.18	0.59	0.14	2.5	5.8	0.0	10	g⁻,t
	0.18	0.22	0.40	0.0	2.4	0.8	5	g⁻,g⁻

The g⁺, g⁻ and t rotamers around the C^{α}–C^{β} bond corresponded to χ^1 torsion angle intervals -60 ± 30, 60 ± 30 and $180 \pm 30°$. Outlined F_r and ΔE values correspond to rotamers around the C^{β}–C^{γ} bond with the lowest value of F_r, so for the same rotamer around C^{α}–C^{β} bond, conformational energy might slightly differ in organic mixture and micelles. Cross-peaks, the volumes of which weakly depend on the side chain orientation, were excluded from F_r's to get a better discrimination of side chain rotamers. Glu⁹ HN resonance was not assigned in the NOESY spectrum of sA in methanol–chloroform (1:1), 0.1 M $LiClO_4$ [12].

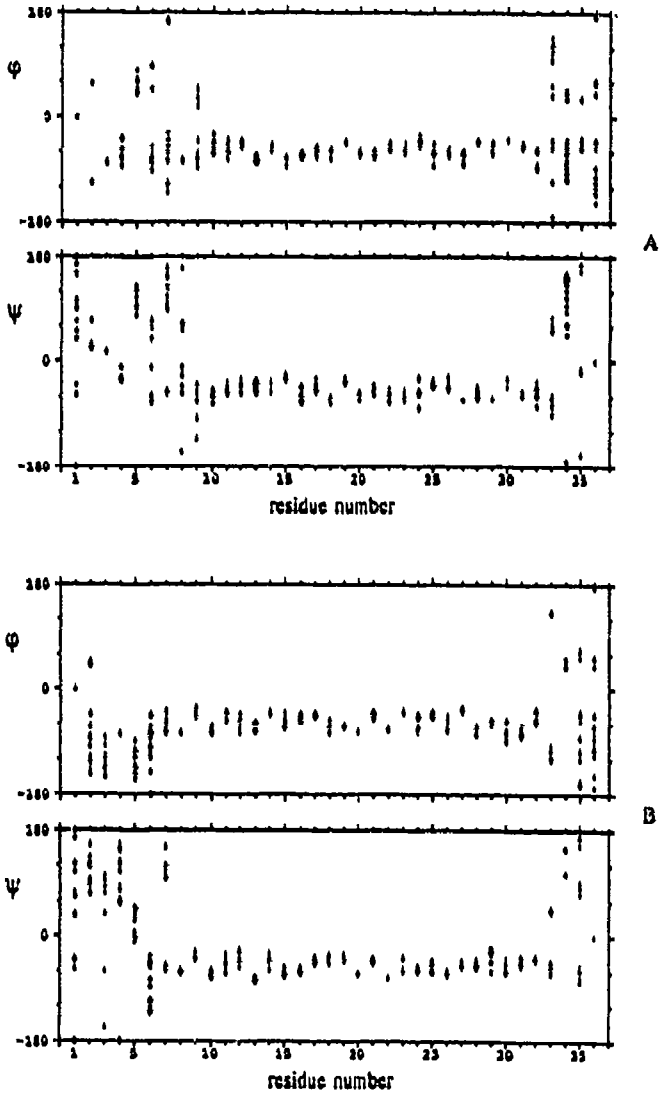

Fig. 2. Torsion angles φ and ψ in 16 final DIANA conformations of sA in (a) methanol–chloroform, 0.1 M $LiClO_4$ solution and (b) SDS-d_{25} micelles plotted versus the residue number.

functions less than 2.9, sum of residual violations of upper distance limits <11 Å, steric repulsing <2 Å and torsion angle constraints <13 Å² were obtained. The maximum values of individual violations of these kinds were less than 0.8 Å, 0.3 Å, and 7 Å in both sets of conformations. After energy minimization these conformations were in good agreement with NOE data as can be seen from the mean values of F_r = 0.25 (SDS) and 0.33 (organic mixture) Å (Table II). This function represents the average difference between the experimental and calculated NOESY cross-peak volumes expressed in terms of distance mismatches and can be considered as an accuracy of the structure determination [11]. The values of RMSD characterize the sA structure from the other viewpoint, which is a variation between the conformations in accordance with the experimental data

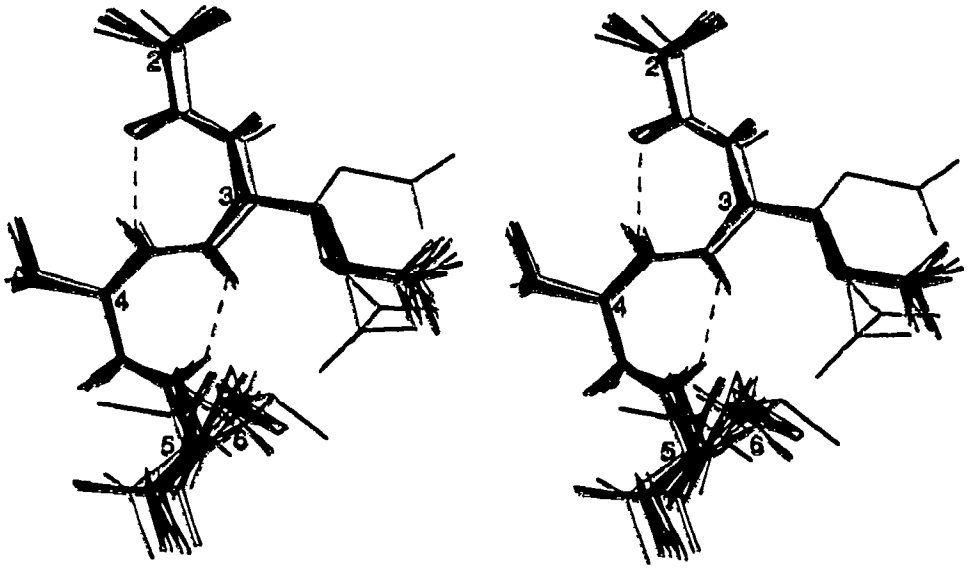

Fig. 3. Stereoview of superpositions for minimum RMSD of the backbone heavy atoms of 12 conformations of the 2-6 fragment of sA in methanol-chloroform (1:1), 0.1 M $LiClO_4$ solution refined by energy minimization with the program CONFORNMR [11,17]. All backbone atoms, all side chain heavy atoms and hydrogen bonds (dashed lines) are shown. Positions of C^{α} atoms are denoted by their corresponding residue number.

(Table II). The α-helical region Pro^{8}–Met^{32} is well defined for sA in the organic mixture as well as in SDS micelles with rather small RMSD of atom's coordinates (see Fig. 2, Table II). The C-terminal region Gly^{33}–Asp^{36} is disordered in both milieus. The N-terminal region Ala^{2}–Gly^{6} in organic mixture has a fixed struc-

Table II

Analysis of the final sets of 16 sA conformations in SDS-d_{25} micelles and methanol-chloroform (1:1), 0.1 M $LiClO_4$

Quantity	SDS-d_{25} micelles	Methanol-chloroform (1:1), 0.1 M $LiClO_4$
Number of NOESY cross-peaks	400	324
Penalty function F_r (Å)	0.25 ± 0.01	0.33 ± 0.02
Number of NOE violations		
with Δr > 1.0 Å	3 ± 1	3 ± 1
with Δr > 0.5 Å	27 ± 4	41 ± 5
ECEPP/2 [19] energy (kcal/mol)	−210 ± 8	−205 ± 12
Pairwise RMSD (Å) of backbone heavy atoms of residues:		
1–36	3.17 ± 1.57	3.92 ± 0.70
2–6	1.44 ± 0.56	0.25 ± 0.12
8–32	0.25 ± 0.07	0.26 ± 0.06
all heavy atoms of residues:		
1–36	3.92 ± 1.57	4.90 ± 0.80
2–6	2.30 ± 0.91	0.61 ± 0.16
8–32	1.08 ± 0.22	1.25 ± 0.23
Pairwise RMSD (Å) of the 16 final NMR conformations to the ECM model [2] of the backbone heavy atoms of residues:		
8–32	1.23 ± 0.17	1.34 ± 0.16
all heavy atoms of residues:		
8–32	2.69 ± 0.34	2.70 ± 0.31

The data are represented as mean value ± S.D. Δr is the distance mismatch corresponding to the deviation of experimental and theoretically evaluated NOESY cross-peak volumes [11,20].

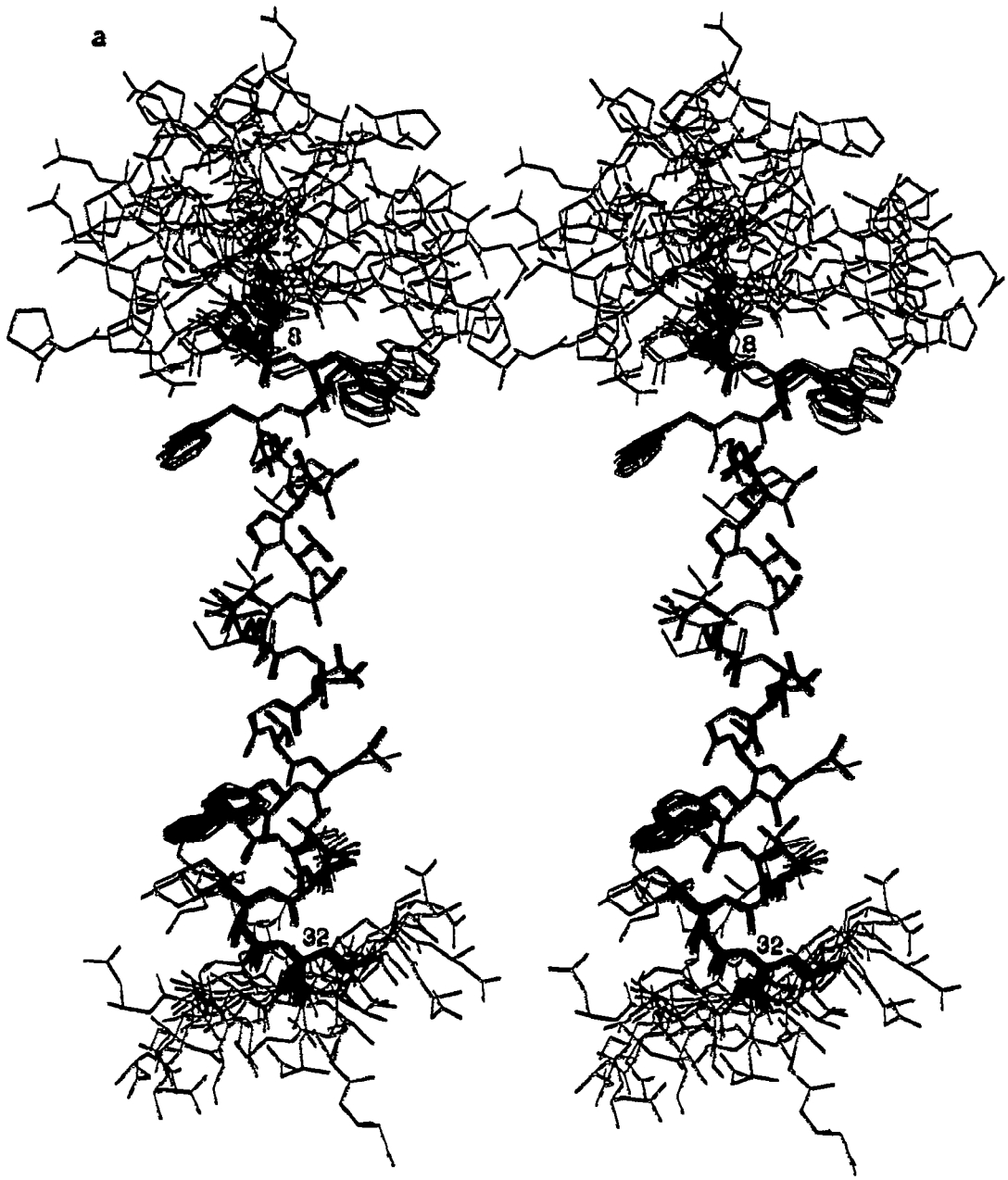

Fig. 4. Stereoview of superpositions of the 16 final conformations for minimum RMSD of the backbone heavy atoms in the 8–32 region of sA in (a) methanol–chloroform (1:1), 0.1 M $LiClO_4$ solution and (b) SDS-d_{25} micelles. All heavy atoms of sA are shown. Residues Pro^8 and Met^{32} are marked by their corresponding numbers.

ture of two consecutive γ-turns as 2 * 2_7-helix (RMSD of 0.25 Å) stabilized by the Ile^4 NH···OC Ala^2 and Thr^5 NH···OC Gln^3 hydrogen bonds (Fig. 3) that slow down the deuterium exchange rates of Ile^4 and Thr^5 amide protons (see Fig. 1). The third γ-turn with participation of the Gly^6 residue seems to be unstable due to faster deuterium exchange of the amide proton of Gly^6 than that of Ile^4 and Thr^5. This region of sA in SDS micelles has an extended structure with RMSD of 1.44 Å for backbone heavy atoms (Table II) and the deuterium exchange rates of amide protons less than 0.5 h (Fig. 1).

The uncertainty of the backbone structure in the Gly^6–Arg^7 hinge region of sA in organic mixture is confirmed by very broad allowed area in φ–ψ maps obtained in the stage of local structure analysis of Gly^6 and Arg^7 residues. The mobility and length of the hinge allows the 2–5 region and α-helical region to adopt a large number of mutual orientations (see Fig. 4a). Contrary to the isotropic milieu of the organic mixture, the

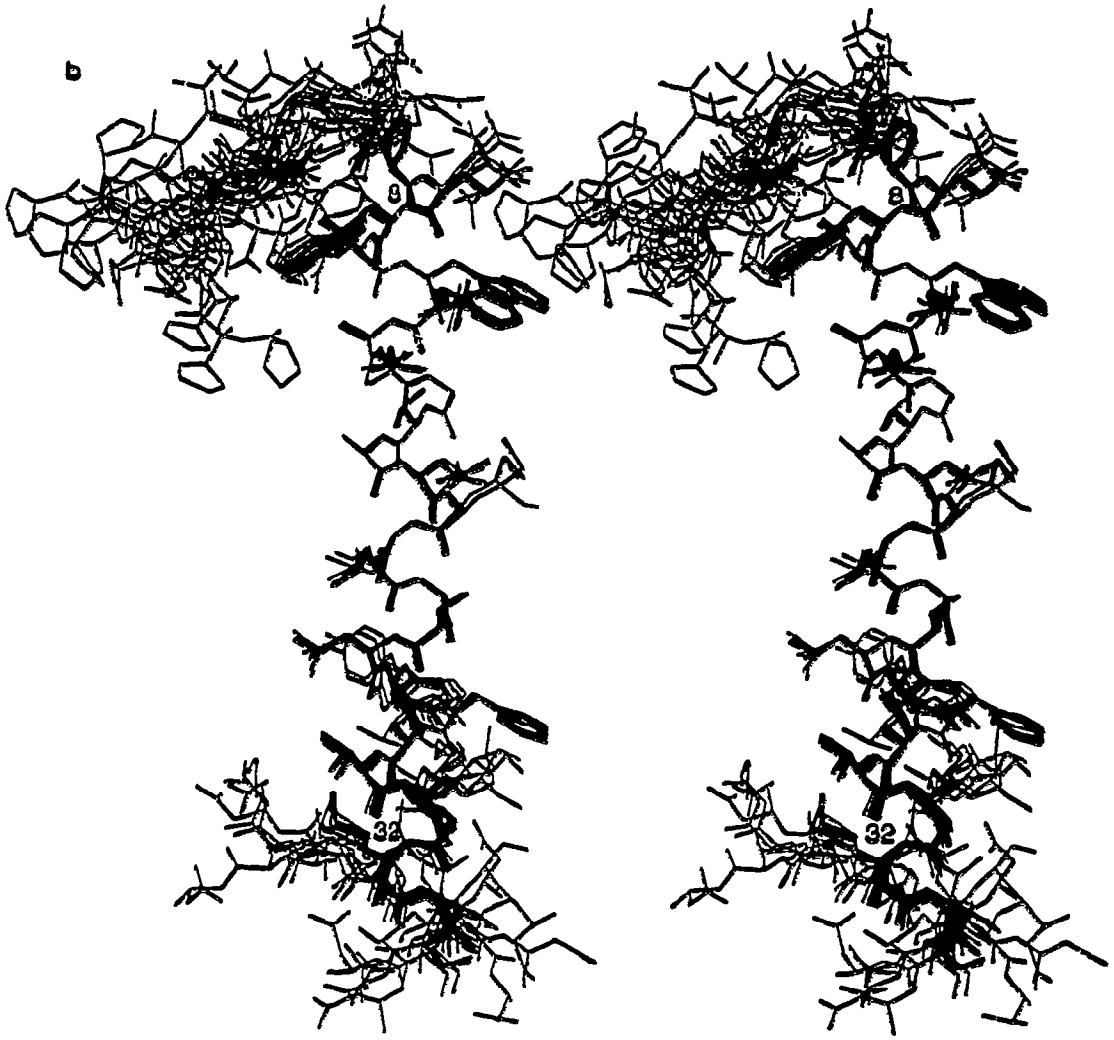

Fig. 4b.

allowed conformational space for Thr[5]-Gly[6]-Arg[7] region of sA in SDS micelles (which is more suitable model for essentially anisotropic native membrane environment) is fairly restricted (see Fig. 2b). This fact in conjunction with the extended conformations of residues Ala[2]-Thr[5] define rather fixed angle of about 70° between axes of α-helix and C^{α}-atom's best fitted line of the Ala[2]-Thr[5] region. The variation of the ψ angle of Arg[7] leads to the veer-like distribution of the 1–6 region (Figs. 2b and 4b) over suggested micelle surface. Alteration of hydrophobic and hydrophilic residues in the 1–7 region implies in the case of the extended conformation that one side of the structure is mostly hydrophobic and the other hydrophilic, providing optimal interactions of the N-terminal 1–7 region of sA with the micelle–water interface. In the purple membrane, the 1–7 region of BR might play the role of an anchor to stabilize the position of the α-helix across the membrane. The 2–6 region of sA in the isotropic milieu of the organic mixture does not have a preferred orientation in respect to the α-helical region (Fig. 4a) even the 2–6 region itself has a rather fixed structure of a $2 * 2_7$-helix with the compound γ-turn pattern of hydrogen bonds [21] (Fig. 3).

The length of 35 Å of the sA α-helical region is enough to penetrate a lipid bilayer. The mobility of most side chains within the α-helical region of sA is restricted: the values of χ^1 were unequivocally determined for 78% (SDS) and 61% (organic mixture) of the α-helical residues (Table I). The rotamer consistent with the NOE data was never energetically unfavorable. The allowed side chain rotamers are identical for most residues of sA in the SDS micelles and the organic mixture which might reflect resemblance of the hydrophobic environment of sA in this two membrane-mimicking milieus. These highly restricted side chains might also play an essential role in the mutual recognition of transmembrane segments of the BR molecule.

A remarkable feature of sA in the organic mixture is a rather low exchange rate of the side chain $H^{\gamma 1}O$ pro-

tons of the Thr residues that made it possible to assign resonances of these protons of Thr^{17} and Thr^{24}. We observed NOESY cross-peaks of $H^{\gamma 1}O$ Thr^{17}/HN Leu^{13}, $H^{\gamma 1}O$ $Thr^{17}/C^{\gamma}H$ Leu^{13}, $H^{\gamma 1}O$ $Thr^{17}/C^{\alpha}H$ Ala^{14} and $H^{\gamma 1}O$ $Thr^{24}/C^{\alpha 1,\alpha 2}H$ Gly^{21} protons. Those cross-peaks define the orientations of the side chain $H^{\gamma 1}O$ groups ($\chi^1 = -60°$) of Thr^{17} and Thr^{24} and make them optimal for the formation of $CO_{i-4}\cdots H^{\gamma 1}O_i$ hydrogen bonds. Formation of these hydrogen bonds causes weakening of the α-helical backbone hydrogen bonds due to competition between the $H^{\gamma 1}O$ and HN groups for a C=O partner that will lead to a relatively fast deuterium exchange for the amide protons of Thr^{17} and Thr^{24} (Fig. 1a). The involvement of a polar $H^{\gamma 1}O$ group in the intramolecular hydrogen bond makes it less exposed to the non-polar milieu surrounding it. For sA in SDS micelles the side chain $H^{\gamma 1}O$ resonances were not observed, but the relatively fast deuterium exchange of the amide protons of Thr^{17} and Thr^{24} (Fig. 1b) might also point to the presence of the above Thr side chain hydrogen bonds in an SDS micelle environment.

According to the ECM data, BR of the purple membrane contains the α-helix located within the 8 to 32 region [2] and the same α-helical region was delineated in the secondary structure analysis of the proteolytic fragment, (1–71)bacteriorhodopsin, in methanol–chloroform (1:1), 0.1 M $LiClO_4$ solution [9]. Thus, the sA and C2 backbone conformations in a membrane-mimicking environment are in good agreement with the ECM model of the native BR structure. It is still difficult to check the obtained conformations of the sA side chains against those reported for the ECM model of BR [2], since this model provides unreliable side chain orientations for most residues [20].

The present results show that NMR spectroscopy might play a unique role in the delineating of the spatial structures of transmembrane fragments of membrane proteins in artificial milieus. These structures might be considered as building blocks of the entire molecules. Thus, NMR spectroscopy should be very instructive for the refinement of the BR spatial structure.

REFERENCES

[1] Ovchinnikov, Yu.A. (1982) FEBS Lett. 148, 179–191.
[2] Henderson, R., Baldwin, J.M., Ceska, T.A., Zemlin, F., Beckmann, E. and Downing, K.H. (1990) J. Mol. Biol. 213, 899–929.
[3] Wüthrich, K. (1989) Science 243, 45–50.
[4] Arseniev, A.S., Maslennikov, I.V., Kozhich, A.T., Bystrov, V.F., Ivanov, V.T. and Ovchinnikov, Yu.A. (1988) FEBS Lett. 231, 81–88.
[5] Maslennikov, I.V., Lomize, A.L. and Arseniev, A.S. (1991) Bioorg. Khim. (USSR) 17, 1456–1469.
[6] Maslennikov, I.V., Arseniev, A.S., Chikin, L.D., Kozhich, A.T., Bystrov, V.F. and Ivanov, V.T. (1991) Biol. Membrany (USSR) 8, 156–160.
[7] Maslennikov, I.V., Arseniev, A.S., Kozhich, A.T., Bystrov, V.F. and Ivanov, V.T. (1990) Biol. Membrany (USSR) 8, 222–229.
[8] Barsukov, I.L., Abdulaeva, G.V., Arseniev, A.S. and Bystrov, V.F. (1990) Eur. J. Biochem. 192, 321–327.
[9] Sobol, A.G., Arseniev, A.S., Abdulaeva, G.V., Musina, L.Yu. and Bystrov, V.F. (1992) J. Biomol. NMR 2, 161–171.
[10] Pervushin, K.V., Arseniev, A.S., Kozhich, A.T. and Ivanov, V.T. (1991) J. Biomol. NMR 1, 313–322.
[11] Lomize, A.L., Pervushin, K.V. and Arseniev, A.S. (1992) J. Biomol. NMR, in press.
[12] Pervushin, K.V., Sobol, A.G., Musina, L.Yu., Abdulaeva, G.V. and Arseniev, A.S. (1992) Mol. Biologia (USSR), in press.
[13] Abdulaeva, G.V., Sychev, S.V. and Tsetlin, V.I. (1987) Bioorg. Khim. (USSR) 4, 1254–1268.
[14] Denk, W., Baumann, R. and Wagner, G. (1986) J. Magn. Reson. 67, 386–390.
[15] Sobol, A.G. and Arseniev, A.S. (1988) Bioorg. Khim. (USSR) 14, 997–1013.
[16] Borgias, B.A. and James, T.L. (1990) J. Magn. Reson. 87, 475–487.
[17] Lomize, A.L., Sobol, A.G. and Arseniev, A.S. (1990) Bioorg. Khim. (USSR) 16, 179–201.
[18] Guntert, P., Braun, W. and Wüthrich, K. (1991) J. Mol. Biol. 217, 517–530.
[19] Nemethy, G., Pottle, M.S. and Scheraga, H.A. (1983) J. Phys. Chem. 87, 1883–1887.
[20] Barsukov, I.L., Nolde, D.E., Lomize, A.L. and Arseniev, A.S. (1992) Eur. J. Biochem., in press.
[21] Milner-White, E.J. (1990) J. Mol. Biol. 216, 385–397.